Chapter 2

The Feasibility of Constructing Super-Long-Span Bridges with New Materials in 2050

Faham Tahmasebinia,
Samad Mohammad Ebrahimzadeh Sepasgozar,
Hannah Blum, Kakarla Raghava Reddy,
Fernando Alonso-Marroquin, Qile Gao, Yang Hu,
Xu Wang and Zhongzheng Wang

Additional information is available at the end of the chapter

http://dx.doi.org/10.5772/intechopen.75298

Abstract

This chapter explores the possibility of designing and constructing a super-long-span bridge with new materials in 2050. The proposed bridge design has a total span of 4440 m with two 330-m end spans and a central span of 3780 m. The height of the two pylons is 702 m, and the deck width is 40 m. The features of this structure include the combination of a suspension bridge and cable-stayed bridge, application of carbon fibre materials, extension of deck width and pretension techniques. Linear static analysis, dynamic analysis and theoretical analysis are conducted under different loading cases. In linear static analysis, the stresses under critical load combinations are smaller than the ultimate strength of the materials. However, the maximum deflection under the dead and wind load combination exceeds the specified serviceability limit.

Keywords: long-span bridges, cables and tendons, materials technology

1. Introduction

The feasibility of designing a super-long-span bridge with new materials in 2050 is studied. Longer bridge spans have the benefits of increased horizontal navigation clearances and reduced risk of ship collisions with piers [1]. The length of very long span suspension and cable-stayed bridges are often limited by the weight of the cables. As spans increase, the cables experience high stresses due to their own self-weight, and the overall structure becomes less

stiff as the stiffening contribution of the deck becomes negligible [1]. Therefore, strong but light-weight materials must be used in the design of super-long-span bridges.

There are many new high-strength materials with low density like carbon fibre with epoxy, graphene oxide and alumina-polymer composites. Some materials have much better mechanical performances than steel or concrete but are only used in some high-tech industries such as aerospace, wind energy and automotive industries due to their high price. By 2050, the new materials are likely to be used extensively in construction due to the reduced cost in the development process of new materials [2]. This paper presents and analyses a super-long-span bridge design which has a total span of 4440 m with 40 m width deck and two 702-m-high pylons. The bridge design is based on the Golden Gate Bridge and a finite element model is created in Strand7 [3] which is a modification to the Golden Gate Bridge model developed by [4]. The central span of the bridge is 3780 m, which is three times the span of the Golden Gate Bridge of 1260 m, while the length of the two end spans is the same at 330 m. Previous studies have been conducted on super-long cable-stayed bridges using carbon fibre reinforced polymer [5] and on long-span suspension bridges using fibre-reinforced polymer [6]. Special techniques are adopted in this design where the bridge combines the advantages of a suspension bridge and a cable-stayed bridge to minimise the deflection of the superstructure and the pylons. The material of the catenary cables and stay cables are changed to a lightweight fibre carbon composite [7] with high stiffness and high strength, and standard carbon fibre is used in the superstructure and the vertical hangers. Finally, the stayed-cables of the bridge are pre-strained in this design.

Carbon nanofibres have cylindrical shapes with graphene layers constructed in the morphology of cones or plates or sheets, with an average diameter of 50–100 nm and an average length of 50–200 um, exceptional thermal and mechanical properties (as high as elastic modulus of 600 GPa, tensile strength of 8.7 GPa, surface area 40 m^2/g), which offer a wide range of applications in the civil engineering discipline (e.g. bridges, roads, railways, tunnels, airports, ports and harbours), and other areas such as aerospace, automotive, sports goods material, and so on. Reinforcement of such new nanocarbons with polymeric materials further boosts their mechanical properties through different fabrication technologies such as wet/hand lay-up/spray lay-up, autoclave curing, filament winding, pultrusion, wet/hand lay-up, and so on. These extraordinary properties of advanced hybrid composites have enabled the design engineers to use them in the renewal of civil infrastructure ranging from the strengthening of reinforced concrete, steel and iron, and for replacement of bridge decks in rehabilitation (seismic repair, strengthen or retrofitting) to the construction of new ultra super-long bridge and building structures with less cost. In 1972, high strength polymeric material roof structure with the shape of an umbrella was manufactured via hand lay-up fabrication process and transported from the UK to be erected at the international airport of Dubai. In 1990s, it was replaced by advanced composites that were made with sophisticated glass fibre-reinforced plastics. Such advanced polymer composites with nanofillers (e.g., nanocarbons, glass fibre) are used for the development of building systems and building blocks using an automated construction system (ACS), which consists of a number of interlocking fibre-reinforced polymers (e.g., aramid) that can assemble into a large number of different efficient civil structures (e.g., 3D form) for use in the construction industry. Some examples of these ACS systems in the area of bridging engineering are Humber Bridge (1410 m span), Aberfeldy Bridge, Iron Bridge and the Bonds Mill Bridge from UK, and Gilman Bridge (450 m span), George Washington Bridge

http://dx.doi.org/10.5772/intechopen.75298

(1067 m span), Golden Gate Bridge (1280 m span) and Wickwire Run bridge from USA, Forth Road Bridge (1005 m span) from Scotland, and Tagus Bridge (1013 m span) from Portugal, and so on. These ACS components are cheaper with durability, light weight, low cost, speed of construction, ease of transportation, and they show superior mechanical properties (e.g., tensile, compression, shear strength) than iron, steel and stone. Therefore, such advanced carbon fibre-reinforced polymer (CFRP) composite materials are promising candidates in the future for the construction of ultra-super-long bridges. It is feasible to develop over 10,000 span stable super-long bridges using new concepts. A new concept of engineering that is used for nanoscale modelling of super-long bridges can be described in following sections.

Finite element models were created in Strand7 [3], and the results show that a maximum deflection of 8.3 m occurs under the combination of dead and wind (G+W) load, which slightly exceeds the AS5100 [11] limit of 6.3 m. Furthermore, a 32.4 m transverse deflection is found under the dynamic wind analysis. Maximum tensile stresses of 1154 and 1152 MPa are observed in the catenary cables and stayed cables, respectively, which are below the tensile strength of 1600 MPa of M55**UD carbon fibre.

2. Structural system

2.1. Structural members

The design of this long-span bridge is based on the Golden Gate Bridge, therefore structural member types are essentially similar to the Golden Gate Bridge, which consists of a bridge deck with a supporting trusses and beams system, two pylons, catenary cables, vertical hangers and stayed cables and eight lanes of vehicle traffic. The design of the central span between the two pylons is based on a typical suspension bridge, while the two edge spans are similar to a cable-stayed bridge. The superstructure spanning between the two pylons is hung by vertical suspenders at 15-m intervals, which is the same as a typical suspension bridge. These vertical hangers carrying the loads on the deck are supported by the catenary cables suspended between the two pylons. Additionally, the stay cables at the two edge spans connecting the top of the pylons and the ends of the bridge are anchored by the abutment anchors at each end of the bridge. The cables directly running from the tower to the deck form a fan-like pattern on a series of parallel lines. Due to the different stress modes on the structural members, different materials are selected for each member based on their properties such as ultimate tensile and compressive strength, density and Young's modulus. The properties of the materials used in the bridge model are listed in **Table 1** [7–9]. The material selection is further discussed for each structural member.

The superstructure of the bridge consists of four major components: the bridge deck, permanent formwork, the cross girder and the deck truss system. The 0.5-m-thick bridge deck is made up of reinforced concrete while the material applied to the rest of the components of the superstructure is standard carbon fibre to reduce the self-weight of the superstructure. **Figure 1** shows the details of the arrangement of the structural members in the superstructure (without the bridge deck). As shown in **Figure 1**, the truss system resisting tensile or compressive force is attached to the cross girders running across the driving direction of the bridge.

Materials	Ultimate tensile/compressive strength (MPa)	Density (kg/m^3)	Young's modulus (GPa)
Steel (Grade 350)	350 (C/T)	8000	207
Reinforced concrete	25.5 (C)	2500	34.5
Standard carbon fibre fabric	600 (T)	1600	70
Carbon fibre composite (M55** UD)	1600 (T)	1650	300 (0°)

Table 1. Properties of the material used in the model.

A 2.5 m-deep UB section is selected for the cross girders to carry flexural loads and then to transfer the loads into the truss system below. The concrete bridge deck sits on top of the truss system and cross girders, and the live load and vertical wind load are directly applied on the top of the bridge deck. Furthermore, the rectangular hollow section cross bracings distribute the loads on the deck onto the cross girders, and they also perform as the tensile reinforcement for the bridge deck above.

The design uses three types of cables: catenary cables, vertical hangers and stayed cables. In the central suspended deck, cables suspended via pylons hold up the road deck, and the weight and the vertical loads are transferred by the cables to the towers, which in turn transfer to the pylons and the anchorages at the end of the bridge. Since all of the cables are in tension, a lightweight carbon fibre or carbon fibre composite should be used in the cables based on material properties in **Table 1**.

Firstly, the catenary cables with a diameter of 2.2 m are suspended between the pylons, with a total cable length of 3915 m and further extend and transfer the loads to the anchorages at the bank. Carbon fibre composite (i.e., M55**UD) is used in the catenary cables. The shape of the catenary cables is determined by selecting an appropriate interpolated shape between the

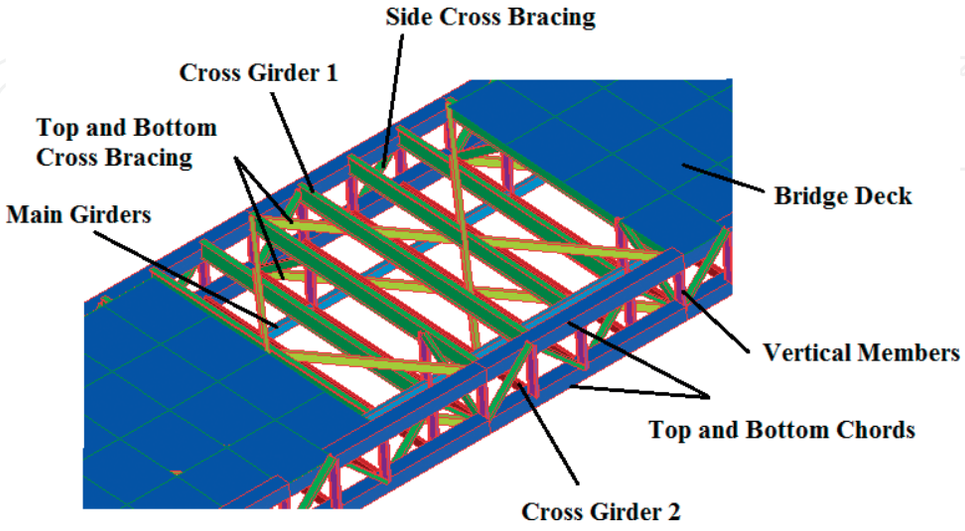

Figure 1. Details of the bridge superstructure.

catenary shape and the parabolic shape. The detailed explanation of this process is introduced in Section 3. The catenary cables are formed by connecting the coordinates that mimicked the shape of the cable, so the cables are segmented instead of smooth. Secondly, there are 252 pairs of vertical hangers at 15-m intervals at the central span. The diameter of the vertical hangers is 0.16 m. Standard carbon fibre is used in vertical hangers due to the relatively low tensile stress. Thirdly, the stayed cables at the two side spans are made up of M55**UD with a diameter of 0.15 m.

Two pylons are also built up at positions which are 330 m from each end of the bridge. The total height of a pylon is 702 m. The superstructure is connected to the pylons at 216 m from the foundations of the pylons. The loads on the catenary cables and the stayed cables are transferred to the pylons as a compressive force; therefore, Grade 350 steel is used as the material of the pylons [10].

The sizes and materials of the structural elements of the long-span bridge are shown in **Table 2**.

2.2. Structural system resisting vertical loads

The vertical loads acting on the bridge mainly consist of the self-weight of the structural members, the live load due to traffic and the vertical wind load. The vertical loads applied to the bridge deck are firstly carried by the reinforced concrete deck through bending, where the deck is directly supported every 5 m by the cross girders (I beams) with web stiffeners. The web stiffeners act to increase the shear capacity of the deep I beams and decrease the chance of shear

Structural elements details	Material	Suggested structural element sizes
Bridge deck	Reinforced concrete	0.5 m thick
Cross girder 1	Standard carbon fibre fabric	2500UB3650
Cross girder 2	Standard carbon fibre fabric	1200×500×50 RHS
Top and bottom chords (blue)	Standard carbon fibre fabric	2000×2000×200 SHS
Top/Bottom cross bracing (yellow)	Standard carbon fibre fabric	1200×500×50 RHS
Side cross bracing (green)	Standard carbon fibre fabric	1000×500×50 RHS
Main girders (blue)	Standard carbon fibre fabric	1400×700×75 RHS
Vertical members (pink)	Standard carbon fibre fabric	1500UB1420
Catenary cables	Carbon fibre composite (M55** UD)	2.2 m diameter
Vertical hangers	Standard carbon fibre fabric	0.16 m diameter
Stayed-cables	Carbon fibre composite (M55** UD)	0.15 m diameter
Pylons	Steel (Grade 350)	16,000×10,000
Pylon diagonal bracing	Steel (Grade 350)	5000×5000
Pylon cross bracing	Steel (Grade 350)	8000×16,000

Table 2. Structural elements for the super-long-span bridge.

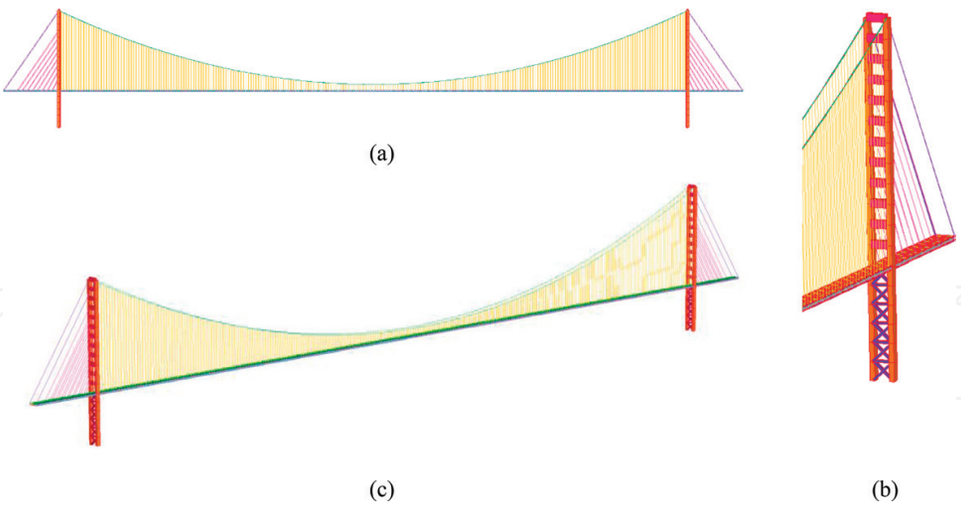

Figure 2. Side views and 3D view of the Strand7 model (a) Longitudinal view, (b) Details of Pylon, (c) 3D view.

buckling in the web. Then the cross girders transfer loads from the bridge deck to the truss system below the deck through bending. In the Strand7 model, the truss members are modelled as rectangular hollow sections to simplify the design. The members of the truss system can only carry axial force, so the top chords are in compression, and the bottom chords are in tension.

The loads on the truss system are spread along the main longitudinal truss members, and further transferred to the vertical hangers which are hanging off the corresponding superstructure every 15 m. These cables carry the loads from the bridge deck up to the catenary cables and the stayed cables through pure tension. On the Golden Gate Bridge, each catenary cable is made up of 27,572 galvanised steel cables which are grouped into 61 cable groups, which are then bunched together to form the 0.92 m diameter cable. For the super-long-span design, the larger diameter of catenary cables and stayed cables requires more galvanised steel cables to group larger cables. These stayed cables are also anchored at the abutments to keep them in tension and to pass the tensile load into the ground through the abutments. The pylons supporting the catenary cables, the stayed cables and the bridge deck are loaded in compression (**Figure 2**).

2.3. Structural system resisting lateral loads

Only wind load is considered as the lateral load acting on the bridge. Because this bridge is very long, the frequency of earthquakes is not consistent with the resonant frequency of the bridge. Therefore, the action of the earthquake load is not significant in this design. For simplicity, it is assumed that the transverse wind load only acts on the superstructure and the pylons. Therefore, the primary system used to resist transverse wind loads consists of the superstructure at the central span which is mainly restrained by the two pylons, the vertical hangers which are further suspended from the catenary cables and two pylons resisting the wind transverse wind load.

2.4. Loads

Dead load (G) accounts for the self-weight of the entire structure, which is calculated by multiplying member dimensions with the corresponding density. The Strand7 model calculated

the structure's mass automatically after input of the material density and geometry. Dead load is then calculated by multiplying the density by the gravitational acceleration.

According to AS5100.2 Bridge Design Codes [11], the live load (Q) applying on the bridge deck is the load resulting from the passage of vehicles and pedestrians, which is SM1600 loading. However, for simplicity, the live load is considered as a pressure acting on the bridge deck in the Strand7 model. The most severe load specified in AS5100.2 is added together and averaged as a pressure load over the bridge deck, resulting in a surface pressure of 10.416 kPa. It is recommended that the Load Influence solver in Strand7 can be used to determine the critical point for the live load and the sensitivity of structure members.

Wind load is the dominant impact on super-long bridges. The first step is to obtain the design wind speed calculated as specified in AS/NZS1170.2 [12], which is derived from regional basic wind speed after adjustment for average return interval, geographical location, terrain category and height above ground. The site wind speed is calculated as:

$$V_{sit,\beta} = V_R M_d \left(M_{z,cat} M_s M_t\right) \tag{1}$$

Since most of the factors vary with different site conditions, and the location of the bridge is not determined yet, by looking at a bridge over Bemboka River in New South Wales, a serviceability design wind speed V_s=37 m/s and an ultimate design wind speed V_u=48 m/s are used in the design. According to AS5100.2 [11], the ultimate design transverse wind load and ultimate vertical wind load are

$$W_t^* = 0.0006\, V_u^2 A_t C_d = 1.935\, A_t \tag{2}$$

$$W_v^* = 0.0006\, V_u^2 A_p C_L = 1.037\, A_t \tag{3}$$

where A_t and A_p are the bridge area in plan, C_d is the drag coefficient, and $C_L = 0.75$ is the lift coefficient. Then the wind load applied on each structure member can be calculated for each structural member. For simplicity, the transverse wind load is assumed to only act on the superstructure and the pylons.

AS5100.2 Clause 23 [11] specifies that for *Ultimate Limit State (ULS)* analysis, the load combinations should include Permanent Effect + Road/rail traffic load and Permanent Effect + Wind load. Therefore, in the static analysis and dynamic analysis, the load combinations of G+Q and G+W are considered.

3. Theoretical analysis

By applying fundamental principles in engineering design, analytical calculations were carried out to determine the optimum cable shape for the suspension bridge and to predict and verify the maximum stresses in the catenary cables and the natural frequency of the structure.

3.1. Optimum cable shape

The shape of a flexible cable under self-weight is a catenary [13]. The equation for a catenary is:

$$y_c = a \times \cosh\left(\frac{x}{a}\right) \tag{4}$$

where the parameter a can be determined once the points through the catenary are known.

Alternatively, when the cables are under heavy load (i.e. the self-weight of cables is negligible compared to the applied uniformly distributed load), then the shape becomes a parabola with the equation:

$$y_p = \frac{w}{2T_0}x^2 + \beta \tag{5}$$

where T_0 is the tensile force in the middle of the cable, w is the uniformly distributed load, and β is the distance between the lowest point of the cable and the top surface of the deck. However, in this design of a super-long-span suspension bridge, neither the self-weight of cables nor the applied uniformly distributed load from the deck can be ignored. Therefore, the resulting shape of the catenary cable is between the shape of a parabola and a catenary [14]. To determine the optimum cable shape that results in minimum deflection for the suspension bridge, an interpolation factor, K, is introduced to determine the final cable shape:

$$y = K \times y_c + (1 - K) \times y_p \tag{6}$$

where $K \in [0, 1]$. Note that the cable shape will be a catenary when K is 1 or a parabola when K is 0.

When only considering dead loads, the normalised maximum deflections of the middle span are plotted against different K values as shown in **Figure 3**. The normalised deflection is equal

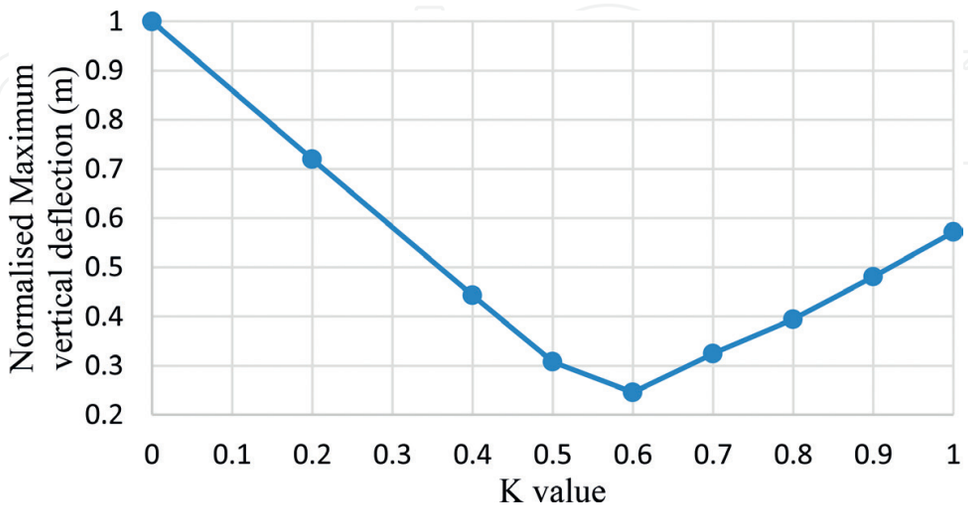

Figure 3. Normalised maximum deflection under self-weight vs. K.

http://dx.doi.org/10.5772/intechopen.75298

to the maximum defection with a specific K value divided by the maximum deflection with K = 0. It is observed that for different K values, the maximum deflections for each case are different, and it reaches a minimum when K is about 0.6. It is also important to note that when the applied load has changed, the optimum K value will change as well. For example, when considering the live load by applying additional uniformly distributed load onto the deck, the optimum value K will increase since the overall load will be closer to a uniformly distributed load where K = 1 (i.e. a parabolic shape will have minimum deflections), so the optimum cable shape would be closer to a parabola. By considering different loading cases while maintaining relatively low deflections, a K value of 0.7 was adopted for the design.

3.2. Maximum tensile stress in main span cables under dead loads

To determine the maximum tensile stress in cables, four assumptions are made to simplify calculations. First, the combination of the self-weights of the cables and the decks is regarded as a uniformly distributed load, which means the consequent cable shape is parabolic. Second, the displacement of the top point of the pylons can be neglected by assuming pin connections between cables and pylons. Third, the deflection of cables under loading is not significant meaning that it will not affect the loads. Fourth, the influence of earth curvature is ignored, which means the gravitational forces are perfectly downwards. The free body diagram of half internal span is shown in **Figure 4**.

From **Figure 4**, T_0 is the horizontal tensile force at the midpoint, w is the uniformly distributed load, L is the total length of internal span, h is the extreme difference of the main cable in the vertical direction and T_{max} is tensile stress at the pylon.

By applying the moment equilibrium at the top right corner, it can be obtained that:

$$\sum M = T_0 \times h - w \times \frac{L}{2} \times \frac{L}{4} = 0 \rightarrow T_0 = \frac{w L^2}{8h} \tag{7}$$

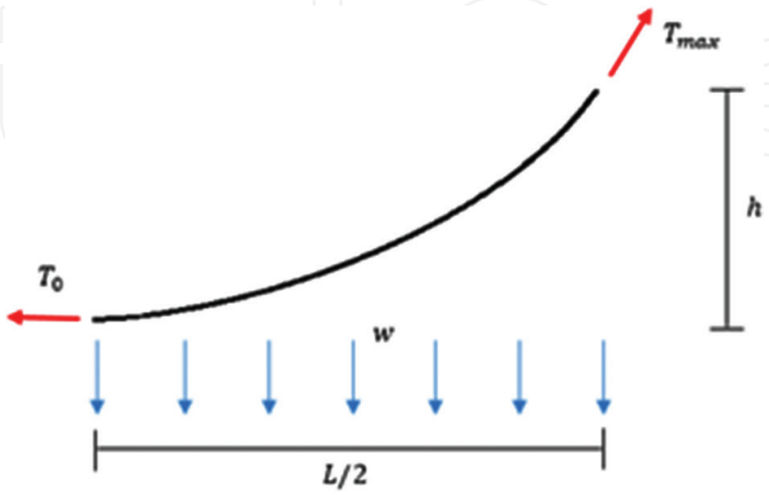

Figure 4. Free body diagram of main cable—Half internal span.

Then, by applying Pythagorean theorem, the T_{max} is obtained:

$$T_{max} = \sqrt{T_0^2 + \left(\frac{wL}{2}\right)^2} = \sqrt{\frac{w^2 L^4}{64 h^2} + \frac{w^2 L^2}{4}} \tag{8}$$

From Strand7, the dead load of the deck and cables is obtained: $w = 485.275\,kN/m$. With $L = 3780$ m, $h = 443.5$ m, the horizontal tensile force is calculated to be $T_0 = 1954.29$ kN, and $T_{max} = 2158.80$ kN. Then, for a cable with diameter D = 2.2 m, the stresses are calculated by dividing the force by the cross-sectional area of cable: $\sigma_0 = \frac{T_0}{A} = 515$ MPa, and $\sigma_{max} = \frac{T_{max}}{A} = 568$ MPa.

3.3. Bridge natural frequency

The natural frequency of bridges is affected by different material and geometric properties:

$$n = f(E, I, \rho, k, L) \tag{9}$$

where E is elastic modulus, I is the second moment of area, ρ is the density of materials, k is the factor depending on the boundary condition and L is the span distance of the bridge.

Since the equation for the natural frequency for a complete representation of the suspension bridge is extremely complicated, a simplified method was adopted under the following three assumptions. First, the oscillation mode will be such that the bridge will deflect in the transverse direction, which is consistent with the first mode determined from the numerical analysis presented. Second, the geometric structure of the deck will be regarded as a simple beam. Third, the cables provide no significant effect on the oscillation frequency in the transverse direction. By applying a simplified equation:

$$n = \frac{K}{2\pi L^2}\sqrt{\frac{EI}{m}} \tag{10}$$

where K is a constant depending on the mode of vibration mode, m is the mass per metre for the deck, then the natural frequency of the first mode is determined to be 0.0212 Hz.

4. Numerical analysis

A detailed finite element model of the structure was created in Strand7 [3], and details of the model are described.

4.1. Mesh and mesh quality

In Strand7, plate elements are used to model the bridge concrete deck, while the remainder of bridge elements use cut-off bars and beam elements. Only the plate elements within the model need meshing as cut-off bars and beam elements in the truss system do not require meshing. However, the node positions of truss members below the bridge deck have already

subdivided the deck plate, resulting in a relatively coarse mesh. Since the bridge deck is not a critical component in the analysis process, the mesh quality of plate elements is not an issue.

4.2. Element types

For the bridge superstructure, the bridge lanes are modelled by plate elements having concrete material properties. The components of the truss system supporting the concrete deck are modelled as beam elements in the shape of I sections or rectangular hollow sections (RHS). In addition, the pylons, pylon diagonal bracings and pylon cross bracings are modelled as B2 elements (beam element) with solid rectangular sections.

The catenary cable is modelled using cut-off bar elements which are connected between nodes with coordinates that are determined by a theoretical analysis using both catenary curve and parabolic curve equations. The optimum cable shape results in an acceptable maximum deflection. The nodes for the catenary cables were imported into the Strand7 model, and were then joined by B2 cut-off bar elements to form the catenary cables. The vertical cables are also modelled by connecting the nodes on the catenary cables and bridge deck by using cut-off bar elements. Similarly, the stay cables are also modelled by connecting the nodes on the pylons and edge span bridge decks with cut-off bars. The reason for selecting cut-off bar is that this type of beam element only allows axial forces and allows users to set the tensile or compressive capacity of the bar. Therefore, all of the cables can be set to have zero compressive capacities.

The nodes on the base of the pylons were completely fixed in all six degrees of freedom, which includes DX, DY and DZ as well as RX, RY and RZ, which is consistent with real structural behaviours with a deep and strong foundation system. Meanwhile, four giant anchors located at the ends of the bridge span are also fully fixed to prevent bridge movements in all directions.

4.3. Solvers used in the analysis

Both the static solver and the dynamic solver are used in the numerical analysis. The deflection of the bridge and the stress within the structure members under dead load, live load, wind load and their combinations are determined by the linear static solver. The non-linear static solver is used to guarantee the maximum stresses within the members are below the yield stress of the corresponding materials.

The Natural Frequency Solver is used to determine the natural frequencies of the bridge based on the results of linear static analysis. Linear static analysis under the G+Q load is conducted first since the tension and compression within structural members would have significant impacts on its natural frequencies. Up to 50 frequency modes are analysed in order to obtain the sufficient mass participation of the bridge.

Once the natural frequency analysis is completed, the harmonic response analysis is performed to determine the mass participation of the bridge and its displacements under wind load. Case factor is set as 1.0 for wind load only, a 5% modal damping is applied in harmonic analysis and all 50 natural frequencies are investigated. The resonance frequency and the corresponding deflection can be obtained in the harmonic response analysis.

Spectral response solver is used to investigate the dynamic response to wind load, with the aid of a power spectral density curve. A 5% modal damping is applied and the results are calculated based on square root of the sum of the squares (SRSS) approach.

5. Structural design

In terms of structural design of the bridge, the capacity is defined as the strength limit state by the critical members which experience maximum axial force, bending moment or shear force. The serviceability limit state is also considered; therefore, the deflections of the deck are checked. In particular, carbon fibre has no yielding behaviours, so there will be no sign of failure in the carbon fibre cables. For members consisting of standard carbon fibre and M55**UD carbon fibre composite, the tensile strength is reduced by 80% due to this brittle nature. For steel members, the section yield stress is factored down to 90% of full yielding. According to the Steel Structures design code AS4100 [8], the nominal section capacity for members subject to axial tension and compression is calculated using the equations:

$$f_t^* = 0.85 \varnothing k_t f_u \tag{11}$$

$$f_c^* = \varnothing k_t f_y \tag{12}$$

Assuming the tensile load is distributed uniformly to the catenary cable, the value of k_t equals to 1. As the catenary cables made of M55**UD carbon fibre composite are only subjected to tensile forces, the factored tensile capacity f_{t_cc} can be obtained as:

$$f_{t\_cc} = 0.85 \times 0.9 \times 1600 = 1224 \text{ MPa} \tag{13}$$

Similarly, for the truss members and vertical cables which are made up of standard carbon fibre, it is assumed that their effective cross-sectional area equals their total cross-sectional area ($k_f = 1$). Therefore, the factored tensile capacity f_{t_c} and compressive capacity f_{c_c} can be obtained as:

$$f_{t\_c} = 0.85 \times 0.9 \times 600 = 459 \text{ MPa} \tag{14}$$

$$f_{c\_c} = 0.9 \times 570 = 513 \text{ MPa} \tag{15}$$

Pylons are made up of Grade 350 steel, where the factored yield capacity f_{c_p} is calculated as:

$$f_{c\_p} = 0.8 \times 350 = 315 \text{ MPa} \tag{16}$$

5.1. Cable design

For bridges with super-long spans, the most challenging and critical members are vertical cables and catenary cables because the dead and live loads acting on the bridge deck are mainly transferred to the vertical cables and further to the catenary cables, which result in large tensile stresses in those cables. As specified above, the vertical cables and catenary cables are cut-off bars, which only resist axial tensile force. The Strand7 linear static analysis results under the G + Q case give the maximum tensile stresses in the cables compared to the capacities in **Table 3**.

For catenary cables, the maximum tensile stress is applied at the end segments near the pylons, which is reasonable since loads on the catenary cables are transferred to the pylons and further to the stayed cables. The last column in **Table 3** is the percentage of maximum applied stress to the tensile capacity. The results show that the current cable design is optimistic as the applied stresses are extremely close to the cable capacity, and the maximum bridge deflection under G+Q is relatively close to the AS5100 [11] limit. However, it is significant to note that the dimension of the catenary cable is relatively large compared to the original design, as it was increased from 1.20 to 2.20 m in diameter. To prove the validity of the Strand7 model, the maximum applied stress in the catenary cables in Strand7 analysis is compared with the analytical results in later sections.

5.2. Deck design

In terms of the deck design, the deck members are divided into two groups: truss members and flexural members. Truss members such as the top and bottom chords resist axial load only, so the tensile and compressive axial strength for each type is compared with the maximum applied axial loads under the most critical load combination (G+Q). Flexural members such as the top and bottom cross girders also experience significant bending moments; thus, the calculated moment section capacity for each type of member is further compared with the maximum applied bending moments under the G+Q case. In particular, for a conservative design, the axial and bending capacities in **Table 4** are factored into capacities.

The last column in **Table 4** indicates the larger percentages of applied axial stress to the axial capacity of critical axial force in terms of tension or compression. All truss members have a

Member type	Member dimensions (m in diameter)	Tensile capacity (MPa)	Maximum stress (MPa)	Capacity (%)
Vertical cables	0.16	459	416	90.63
Catenary cables	2.20	1224	1154	94.28
Stayed cables	0.15	1224	1152	94.11

Table 3. Comparison of tensile capacity to maximum applied stress (suggested design).

Truss members	Geometry	Capacity		Loading		Capacity (%)
		f_{u_t} (MPa)	f_{u_c} (MPa)	Design tension (MPa)	Design compression (MPa)	
Bottom cross girders	1200×500×50 RHS	459	513	53	8	11.5
Top/bottom chords	2000×2000×200 RHS	459	513	72	32	15.7
Top/bottom cross bracings	1200×500×50 RHS	459	513	29	15	6.3
Side cross bracings	1000×500×50 RHS	459	513	208	285	55.6
Main girders	1400×700×75 RHS	459	513	10	10	2.2
Vertical bracings	500UB667	459	513	66	17	14.4
Top cross girders	2500UB3650	459	513	10	19	3.7

Table 4. Design of deck truss members based on axial capacity (current design).

percentage of capacity less than 100%, which indicates that this design satisfies the strength limit state requirements. However, except for side cross-bracing members, the percentages of capacity for other truss members are less than 15%, which means that these members are over-conservative. Hence, the geometries for those members can be adjusted to achieve a more economical design.

For the deck flexural members under bending, the section capacity can be obtained by:

$$M = \frac{\sigma y}{I} \tag{17}$$

In terms of the section modulus and the axial compression capacity, the section capacity for the top and bottom cross girder and top and bottom chords is calculated as follows (**Table 5**):

$$M_{t\_g} = 0.262 \times 459 \times 10^3 = 1.203 \times 10^5 \text{ kNm} \tag{18}$$

$$M_c = 0.787 \times 459 \times 10^3 = 3.612 \times 10^5 \text{ kNm} \tag{19}$$

Flexural members	Geometry				Capacity		Loading	Capacity (%)
	Area (m^2)	Ix (m^4)	y (m)	Z_x (m^3)	f_{u_c} (MPa)	Section capacity (kNm)	Design moment (kNm)	
Top cross girder	0.465	0.328	1.25	0.262	459	1.203×10^5	12,025	10
Top/bottom chords	1.440	0.787	1.00	0.787	459	3.612×10^5	315,000	87.2
Bottom cross girder	0.160	0.028	0.60	0.046	459	0.21×10^5	725	3.5

Table 5. Design of deck flexural members based on moment section capacity (current design).

http://dx.doi.org/10.5772/intechopen.75298

$$M_{b\_g} = 0.046 \times 459 \times 10^3 = 0.21 \times 10^5 \text{ kNm} \quad (20)$$

Similarly, all deck flexural members have a percentage of capacity less than 100% while for the top and bottom cross girders the value is below 15%, so the member geometries are necessarily optimised to achieve a more economical design.

6. Results and discussion

6.1. Static analysis

Using the linear static solver available in Strand7, the suspension bridge is assessed in terms of deflections and stresses under the G+Q and G+W cases. As specified in AS5100.2 [11], the ratio of the allowable vertical deflection or transverse deflection over the length of the span is $\frac{1}{600}$, which corresponds to a maximum deflection of 6.3 m. The allowable deflections are further compared with the results in Strand7 analysis.

6.1.1. Dead load + live load

The deflection contour of the suspension bridge under the combination of dead and live loads is shown in **Figure 5**. The maximum vertical deflection occurs at the middle of the central span, which is around 8.3 m downwards. The vertical deflection exceeds the allowable deflection limit, which is 6.3 m, hence more techniques are required to further decrease the vertical deflection.

In terms of the stresses shown in **Figure 6**, the maximum stresses occur in the catenary cables and stay cables, with the values of 1154 and 1152 MPa respectively. As calculated in Section 5, the carbon fibre composite (M55**UD) used in catenary and stay cables have a factored tensile capacity of 1224 MPa and can sustain the load without failure. Additionally, the vertical cables within the central span have relatively small stress at around 400 MPa, which is below the factored tensile capacity of 459 MPa.

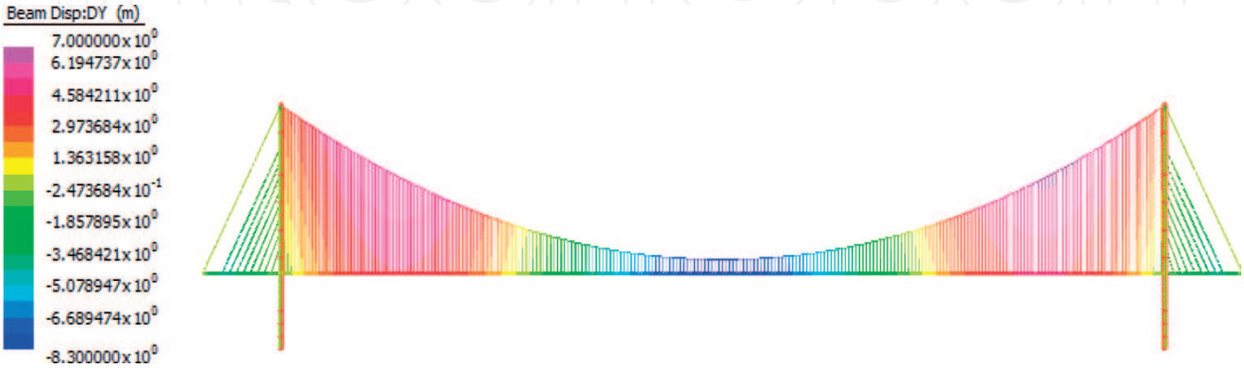

Figure 5. Vertical deflection contour under dead + live load.

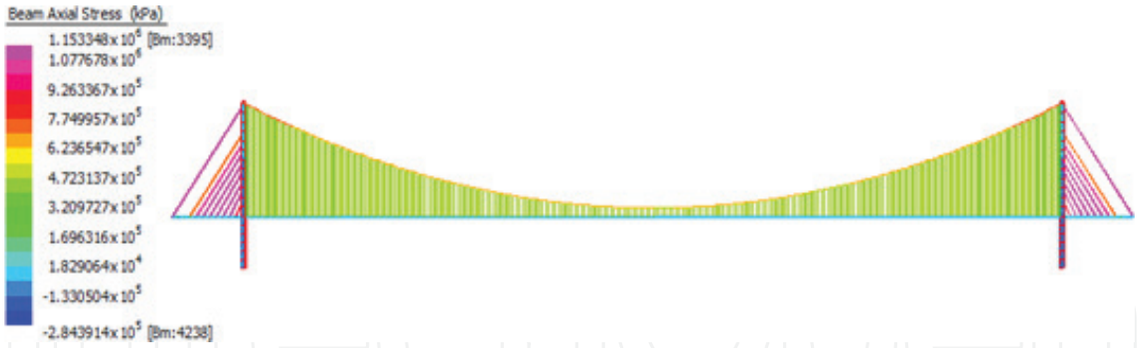

Figure 6. Beam axial stress (kPa) contour under dead and live load combination (G+Q).

6.1.2. Dead load + wind load

A horizontal wind load is applied onto the deck system and pylons. Under linear static analysis, the transverse deflection contour of the "Dead +Wind" loading case is shown in **Figure 7**.

It is found that the transverse deflections at the edge span and the central span near the pylons are very small, and the maximum transverse deflection of 30.9 m occurs at the mid-span of the central span. The transverse deflection under the "Dead load + Wind load" case exceeds the allowable value of 6.3 m, since the out of plane stiffness of the deck is insufficient via the lateral wind load. Therefore, the deflection under the "Dead load + Wind load" case is not satisfactory, and further methods should be considered to reduce the transverse deflection such as improving the stiffness of the deck.

In terms of the stress contours shown in **Figure 8**, the maximum stresses in this case are much lower than the stresses under the "Dead load + Live load" case which indicate that the "Dead load + Wind load" case is not the most critical case for element stresses. Hence the structural elements sufficiently sustain the loads without failure under the "Dead load + Wind load" case.

The catenary cable stress at the mid-span from the Strand7 analysis is compared to the analytical results. Under the "Dead load + Live load" case, the maximum catenary cable stress at the mid-span is 714 MPa, which is located at the region near the pylons, and the horizontal stress at the midpoint of the central span is 646 MPa from Strand7 linear static analysis. **Table 6** shows that there is a 20% difference between the numerical and analytical results.

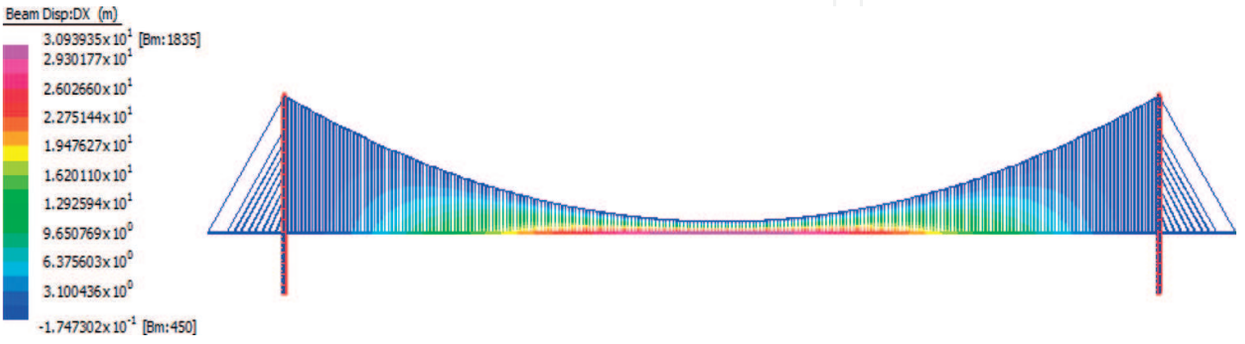

Figure 7. Transverse deflection contour under dead load and wind load.

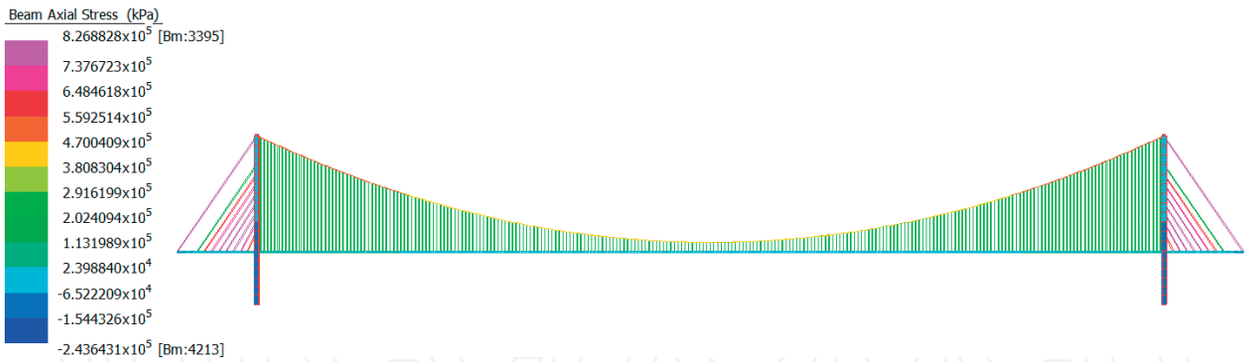

Figure 8. Beam axial stress (kPa) contour under dead and wind load combination (G+W).

6.2. Natural frequency analysis

Natural frequencies of the bridge are solved by Strand7 based on a linear static analysis result under the "Dead load + Live load" case since wind impact is significant when the bridge is in service. Up to 50 different modes of natural frequencies are solved.

In the first mode with a frequency of 0.00338 Hz, the bridge deforms horizontally in a single curvature shape. In the second mode, the bridge deforms horizontally in a double curvature shape, where the frequency is 0.06001 Hz, and in the third mode, the bridge deforms vertically in a double curvature shape, where the frequency is 0.071586 Hz. Further natural frequency modes with higher frequencies are not considered as critical as the first three modes, but the harmonic response solver will be used to investigate the wind impact of these modes to find the most disastrous wind speed.

6.3. Harmonic response analysis

Based on the previous solved natural frequencies, the harmonic response analysis runs under the "wind load only" case with 5% modal damping. **Figure 9** shows that the first mode is the most critical case, since at 0.00338 Hz, the bridge is under resonance and there is a relatively large transverse displacement of 47.6 m at the mid-span of the bridge. Specifically, the wind load is applied as steady sinusoidal force at various frequencies, where each cycle of loading exerts additional energy and increases the vibration amplitude. In this case, when the wind blows in the same frequency as the first natural frequency mode (0.00338 Hz), the bridge is under resonance where the maximum response amplitude occurs and the transverse displacement reaches 47.6 m. Therefore, the super-long bridge is considered to fail when the wind frequency coincides with the first mode of frequency of the bridge. However, the real behaviour of wind loading is further explored in Section 6.4.

	Numerical	Analytical	Difference (%)
Tensile stress near pylons (MPa)	714	568	20.4
Tensile stress at midpoint (MPa)	646	515	20.3

Table 6. Comparison of numerical and analytical catenary cable stresses.

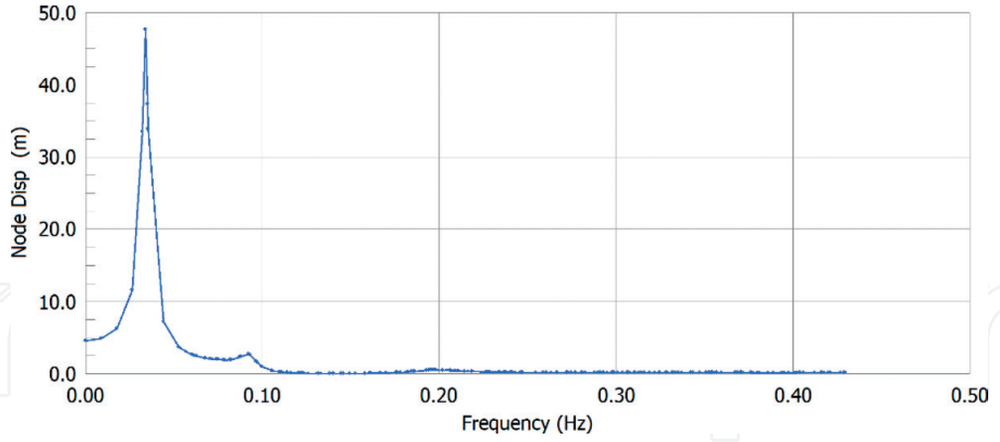

Figure 9. Frequencies vs. nodal displacement (D_x) at the mid-span.

6.4. Spectral response analysis

The linear elastic response of a super-long bridge subjected to a particular wind loading in Australia can be assessed by the "Spectral Response Solver" in Strand7, where the input for dynamic wind analysis can be expressed in terms of Power Spectral Density (PSD) curves [3]. The PSD curve (Davenport's equation) can be expressed as:

$$S_u(n) = 4\,k\,V^2\,\frac{x^2}{n\,(1+x^2)^{\frac{4}{3}}} \tag{21}$$

where $S_u(n)$ is the wind speed power spectral density, n is the frequency, V is the hourly mean wind speed at a 10-m height from the ground, $x = \frac{1200\,n}{V}$ and k is the roughness parameter. As a result, the equation for the Wind Force PSD is plotted as the factor vs. frequency graph in Strand7 and shown as **Figure 10**.

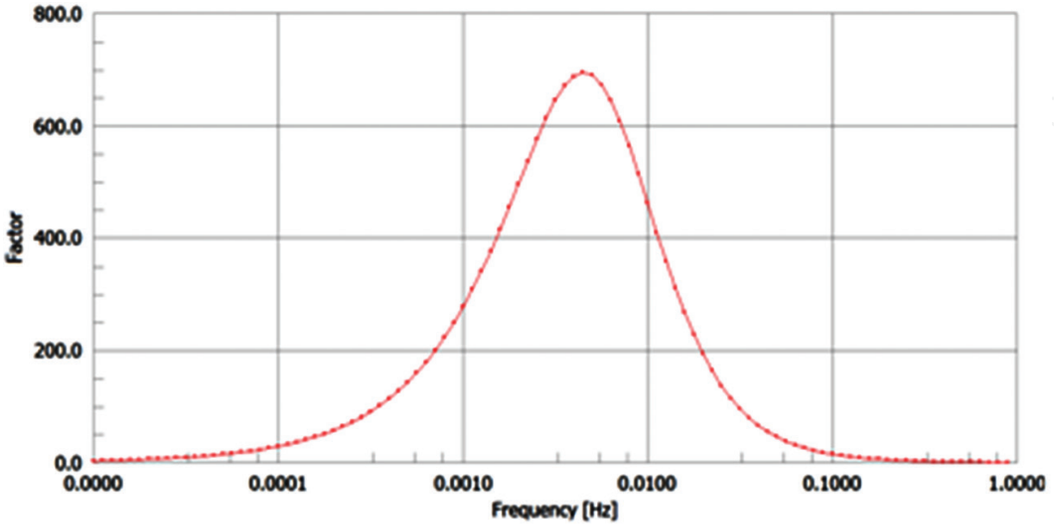

Figure 10. Factor vs. frequency graph for spectral response wind analysis.

http://dx.doi.org/10.5772/intechopen.75298

Figure 10 indicates that the wind load factor changes with wind frequencies and the largest wind load factor occurs when the wind frequency is approximately 0.0045 Hz. Based on the factor vs. frequency graph, the natural frequency of the bridge and applied wind pressure, the "Spectral Response Solver" is run and the result is calculated by the square root of the sum of the squares (SRSS) method in which the coupling among different modes is neglected. In addition, 5% modal damping is applied in the analysis. The result of transverse displacement is shown in **Figure 11**.

The result shows that a maximum transverse deflection of 32.4 m occurs at the mid-span, which is greater than the transverse deflection of 30.9 m obtained from linear static analysis. This phenomenon is reasonable because when the bridge natural frequencies coincide with the heavily factored wind frequencies, the wind impact is severely magnified. As the 32.4 m transverse deflection exceeds the AS5100 limit of 6.3 m, the serviceability criterion is not satisfied. The reason is that the out of plane stiffness of the bridge is insufficient to resist wind forces in this super long bridge. Therefore, further approaches are necessary to increase the lateral stiffness such as increasing the deck width and increasing the depth of the truss system.

6.5. Carbon fibre cost

Standard and ultra-high stiffness carbon fibres are mainly made for high-tech industries like the aerospace industry. They are very expensive and used in specialised applications such as aerofoils. The price for the ultra-high stiffness is $2000 USD per kg [15], whereas standard carbon fibre was $22 USD per kg in 2013 [15]. Currently, ultra-high stiffness is not economical for civil infrastructure. However, **Figure 12** shows the forecast cost of standard carbon fibre. The cost in 2017 is approximately $12 USD per kg, and it has dropped significantly compared to the price in 2013. **Figure 12** shows that the decreasing price trend could be approximated to an exponential function as:

$$cost = k \times e^{-0.187 \times year} \tag{22}$$

where k depends on the year of interest. Based on the same trend, in 2050, the cost of standard carbon fibre would be $0.02 USD per kg and the price of carbon fibre composite would be $1.26 USD per kg, which are even cheaper than the price of steel now of $1.60 USD per kg

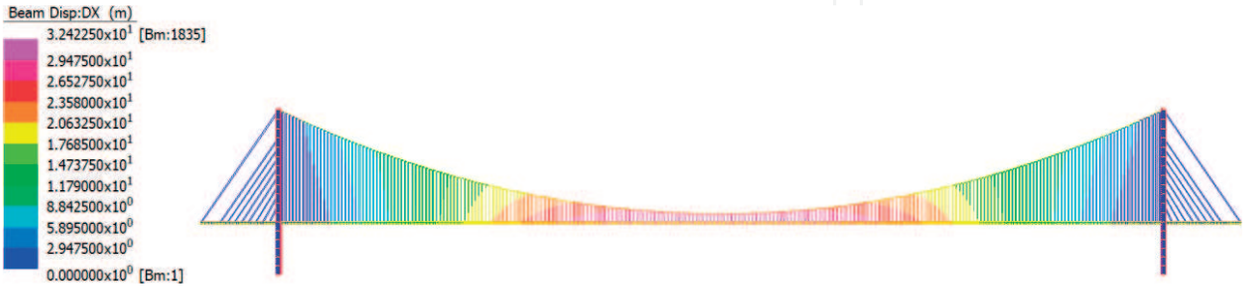

Figure 11. Transverse deflection contour under wind load (spectral response analysis).

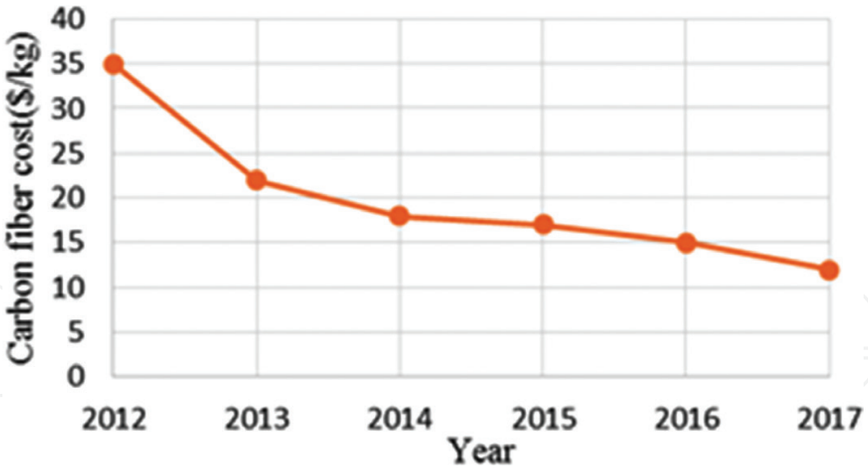

Figure 12. Carbon fibre cost forecast (USD).

[15]. Therefore, carbon fibre could be widely used in civil construction, and this design of a super-long-span bridge may be cost-effective to construct in 2050.

7. Conclusions

The proposed super-long-span bridge design has a total span of 4440 m with two 330-m-long end spans and a central span of 3780 m. Each pylon is designed to be 702 m high, and deck width is 40 m.

M55**UD carbon fibre is adopted for catenary cables and stayed cables because it has higher tensile strength and elastic modulus compared to steel. Standard carbon fibre with a high strength-to-weight ratio is used in the deck system and vertical cables to achieve a lighter self-weight and higher strength capacity. A new iterative technique is introduced and developed to determine the optimum cable shape to minimise the deflections by introducing a K factor. Another innovative design technique, the combination of a cable-stayed and suspension structure, is adopted to balance the deflections of the end and the central bridge spans. A pretension technique is also used in the stayed-cable design.

Overall, in the static analysis, the stresses found under the G+Q and G+W load cases are lower than the capacities of the materials, and the strength requirements are satisfied. However, the maximum deflections under static and dynamic analysis do not meet the criteria for the AS5100 limit of 6 m displacement, with an 8.3 m vertical deflection under the G+Q loading case, a 30.9 m transverse displacement under the G + W static analysis, and a 32.4 m transverse displacement observed in the wind dynamic analysis. Although standard carbon fibre and carbon fibre composite are currently very expensive, the price is expected to drop significantly by 2050 based on recent trends.

Further research is recommended to reduce the transverse deflection by considering increasing the lateral stiffness of the bridge. Additionally, the development of finite element models

with more optimised structural members, section sizes and geometries are recommended to reduce the vertical deflections as well as the total cost of the bridge.

Author details

Faham Tahmasebinia[1,2]*, Samad Mohammad Ebrahimzadeh Sepasgozar[3], Hannah Blum[1], Kakarla Raghava Reddy[1], Fernando Alonso-Marroquin[1], Qile Gao[1], Yang Hu[1], Xu Wang[1] and Zhongzheng Wang[1]

*Address all correspondence to: faham.tahmasebinia@sydney.edu.au

1 School of Civil Engineering, The University of Sydney, Sydney, NSW, Australia

2 School of Mining Engineering, The University of New South Wales, Sydney, NSW, Australia

3 Faculty of Built Environment, The University of New South Wales, Sydney, NSW, Australia

References

[1] Clemente P, Nicolosi G, Raithel A. Preliminary design of very long-span suspension bridges. Engineering Structures. 2000;**22**(12):1699-1706

[2] Shama Rao N, Simha TGA, Rao KP, Ravi Kumar GVV. Carbon Composites are Becoming Competitive and Cost Effective. 2014. White paper from www.infosys.com

[3] Strand7 v2.4.6. Sydney, Australia: Strand7 Pty Limited; 2015

[4] Game T, Vos C, Morshedi R, Gratton R, Alonso-Marroquin F, Tahmasebinia F. Full dynamic model of Golden Gate Bridge. In: AIP Conference Proceedings, Vol. 1762(1). AIP Publishing; 2016, August. p. 020005

[5] Zhang XJ. Mechanics feasibility of using CFRP cables in super long-span cable-stayed bridges. Structural Engineering and Mechanics. 2008;**29**(5):567-579

[6] Yang Y, Wang X, Wu Z. Evaluation of the static and dynamic behaviours of long-span suspension bridges with FRP cables. Journal of Bridge Engineering. 2016;**21**(12):06016008

[7] ACP Composites Inc. Mechanical Properties of Carbon Fiber Composite Materials, Fiber/Epoxy resin (120°C Cure). [Online]. 2010. Available at: https://www.acpsales.com/upload/Mechanical-Properties-of-Carbon-Fiber-Composite-Materials.pdf [Accessed: 29 June 2017]

[8] Standards Australia. S4100.2:2016 Steel Structure. Sydney, Australia: Standards Australia; 2016

[9] Bluescope Steel. HA350 steel Datasheet Datasheets. 2017. See http://steelproducts.bluescopesteel.com.au/category/datasheets [Accessed: 29 June 2017]

[10] Grässel O, Krüger L, Frommeyer G, Meyer LW. High strength Fe–Mn–(Al, Si) TRIP/TWIP steels development—Properties—Application. International Journal of Plasticity. 2000;**16**(10):1391-1409

[11] Standards Australia. AS5100.2:2017 Bridge Design, Part 2: Design Loads. Sydney, Australia: Standards Australia; 2017

[12] Standards Australia. AS/NZS1170.2:2011 Structural Design Actions: Wind Actions. Sydney, Australia: Standards Australia; 2011

[13] Byer O, Lazebnik F, Smeltzer DL. Methods for Euclidean Geometry. U.S.A: MAA; 2010

[14] Kunkel P. Hanging With Galileo. Whistler Alley Mathematics [Online]. 2006. Available at: http://whistleralley.com/hanging/hanging.htm. [Accessed: 27 March 2016]

[15] Prince Engineering. Carbon Fiber used in Fiber Reinforced Plastic (FRP). [Online]. 2013. Available at: http://www.build-on-prince.com/carbon-fiber.html#sthash.gBoq2sJ6.dpbs. [Accessed: 3 July 2017]